Growth and Characterization of $L1_0$ FePt and CoPt $\langle 001 \rangle$ Textured Polycrystalline Thin Films

Sangki Jeong, Michael E. McHenry, and David E. Laughlin

***Abstract*—Thin $\langle 001 \rangle$ textured FePt and CoPt polycrystalline films (5 nm) were deposited with an MgO polycrystalline underlayer on an oxidized Si substrate followed by a Rapid Thermal Annealing (RTA) process. Structural analysis indicated the samples to be fully ordered after 10 minutes (min) of RTA at 700 °C. The magnetic hysteresis exhibited strong perpendicular anisotropy and a coercivity (H_c) between 6 and 8 kOe. The measured and simulated angular dependence of H_c and remanent coercivity (H_{rc}) showed the possibility of domain wall motion or incoherent rotation. δM curves demonstrated strong intergranular exchange coupling. MFM observations showed domain sizes to be 100–200 nm. Activation volumes (V_{act}) were found to be ~ 0.4–0.5×10^{-18} cm^3. The temperature dependence of the coercivity (H_c) indicated a weak pinning mechanism.**

***Index Terms*—FePt and CoPt, perpendicular magnetic anisotropy, reversal mechanism, thin films.**

I. Introduction

FePt AND CoPt thin films have received attention for their potential application in high density recording media [1], [2]. Fine grains with preferred orientations of c-axes and magnetization reversal by a rotation mechanism will determine the feasibility of these materials in recording media applications [1]–[3]. There have been reports on epitaxial $L1_0$ films [1] using single crystalline MgO substrates that exhibited perpendicular anisotropy although this has not proved practical for applications. It has been found that a polycrystalline MgO underlayer film is beneficial in the control of the c-axes orientations of $L1_0$ CoPt and FePt films [4], [5]. The different texture is developed after the annealing process and depends on the thickness of $L1_0$ films. Interestingly, 5 nm FePt and CoPt films MgO underlayers exhibited preferential growth of c-axes perpendicular to the film surface after annealing. On the other hand, the films with the thickness of 20–40 nm showed predominance of in-plane c-axes and are presented in [5]. Here, the structure and reversal mechanism of 5 nm thick films are discussed based on the detailed characterization.

II. Experimental Procedure

FePt, CoPt and MgO films with a SiO_2 capping layer were deposited on oxidized Si substrates at ambient temperature by RF diode sputtering. An alloy target of CoPt, an MgO target, and Pt chips on an Fe target were used to synthesize the films. The samples were annealed in a rapid thermal annealer under an Ar flow. Magnetic properties were measured using Vibrating Sample Magnetometry (VSM) and Alternating Gradient Force Magnetometry (AGFM) in maximum fields of 14 to 20 kOe. The crystal structures and microstructures were examined by XRD (Cu K_α radiation) and Transmission Electron Microscopy (TEM). The magnetic domain patterns were observed by means of Magnetic Force Microscopy (MFM). The temperature dependence of the H_c was obtained by VSM measurement from room temperature to 473 °K. The chemical compositions of the films were determined to be about $Co_{46}Pt_{54}$ and $Fe_{55}Pt_{45}$ by an X-ray fluorescence method. The thickness of films were fixed at $\sim$5 nm. Magnetic properties were measured for the samples after RTA at 700 °C for 18 minutes.

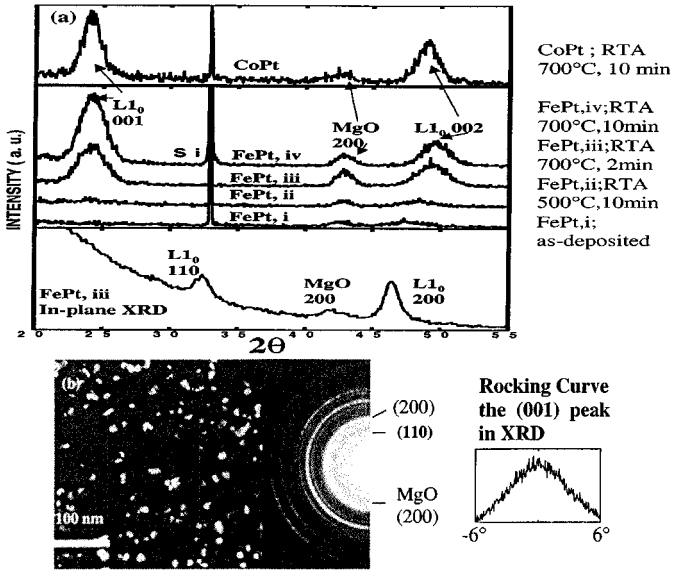

Fig. 1. (a) X-ray $\theta/2\theta$ diffraction spectra of the CoPt and FePt 5 nm films, In plane $\theta/2\theta$ XRD with the grazing incidence angle 2°; (b) Dark field image, SAD patterns in TEM, and a rocking curve in XRD for the FePt samples after RTA at 700 °C for 18 minutes.

III. Results and Discussion

Fig. 1 shows an XRD spectra, a Selected Area Diffraction pattern (SAD) and a dark field image in TEM. The FePt films annealed at 500 °C for 10 min. exhibited an (002) $L1_0$ peak mixed with an FCC (200). In-plane XRD ($\theta/2\theta$ scans) confirmed the absence of the FCC phase in films and only perpendicular structural variants in FePt films annealed at 700 °C for

Manuscript received October 13, 2000.

This work was supported by the Data Storage Systems Center at CMU under Grant ECD-89-07068 from the National Science Foundation and also supported in part by MURI at CMU.

The authors are with the Materials Science and Engineering Department, Carnegie Mellon University, Pittsburgh, PA 15213 USA (e-mail: sjeong@andrew.cmu.edu).

Publisher Item Identifier S 0018-9464(01)07453-2.

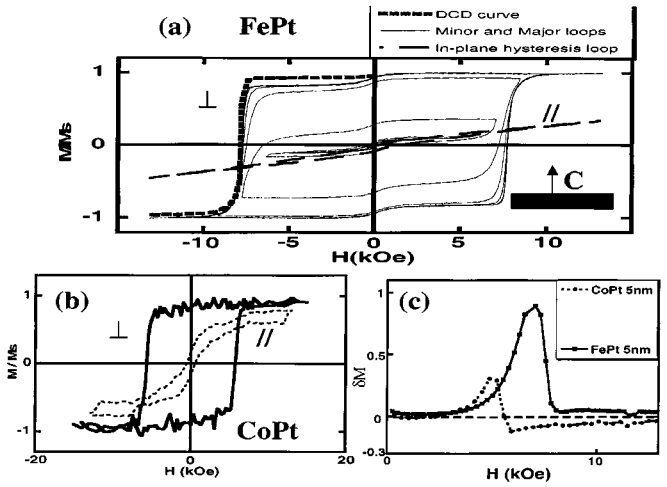

Fig. 2. (a) Major and minor hysteresis loops of FePt samples. DC demagnetization (DCD) curve; (b) The magnetic hysteresis loops of CoPt films; (c) δM curves for the samples in (a) and (b), $\perp$; // in-plane, $\perp$ perpendicular direction to film surface.

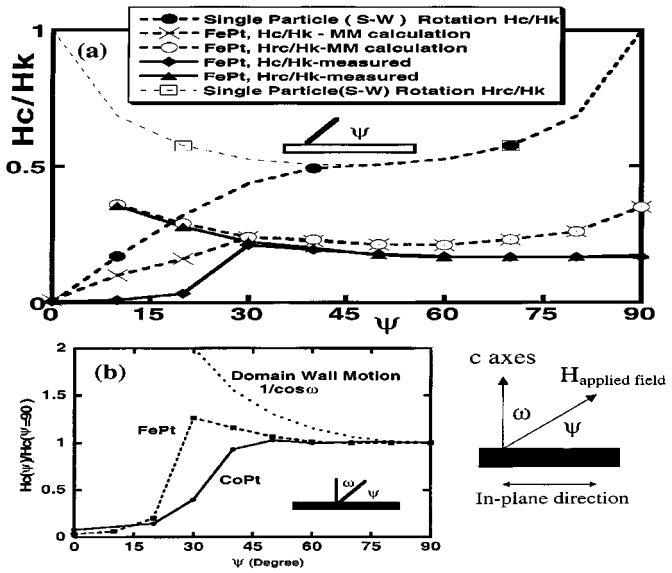

Fig. 3. (a) Comparison between the measured and calculated angular variation in FePt 5 nm films. Angular dependence of H_c and H_{rc} for FePt samples. All measured values are normalized by H_k measured from the hard axis. The calculated values (normalized by H_k) were based on Stoner–Wohlfarth model (S–W) and micromagnetic (MM) simulation [8], [9]. α (damping coefficient) $= 1$ is chosen in all MM calculations.; (b) Measured angular variation of H_c for CoPt and FePt 5 nm films. All values are normalized by H_c in the perpendicular direction to the films surface. Domain wall motion ($1/\cos\omega$ law) was indicated.

2 minutes. The detailed discussions on the effects of structural variants and FCC phase on XRD patterns can be found in References [4], [5]. CoPt had a similar spectrum as the SAD pattern for FePt films where only a $L1_0$ (110) super-lattice reflection was observed. The SAD pattern of CoPt films exhibited a very weak (001) as well as a strong (110) reflection. The calculated intensity ratios of I_{001}/I_{002} (XRD, conventional $\theta/2\theta$ scans) for fully ordered FePt and CoPt are ~2.3 and 1.9 for FePt and CoPt, respectively, considering the product of the structure, Lorentz-polarization, temperature and absorption factors. The measured intensity ratio of FePt after 10–18 min. at 700 °C was slightly higher, which is inferred to be fully ordered (the measured $I_{001}/I_{002} \sim 2.4$–2.5). CoPt after the same annealing also showed predominance of ordered phase (S~0.86, the measured I_{001}/I_{002} ~1.65, neglecting small fraction of in-plane variants). The average grain size in FePt is ~10 nm after RTA at 700 °C for 18 min. A strong perpendicular anisotropy is seen in FePt and CoPt films as shown in Fig. 2(a) and (b). The reason why very thin films favor $\langle 001 \rangle$ texture is not clear and is the subject of ongoing works. However, c/a ratio of FePt films (based on conventional $\theta/2\theta$ and in-plane $\theta/2\theta$ scans) is ~0.94 which is smaller than the values (~0.96) found in bulk and thick films [4]–[6]). Therefore, the strain energy between the underlayer and magnetic films might be a possible explanation since the lattice parameter of MgO is ~5–6% larger than that of magnetic films. Fig. 2(a) illustrates the normalized major and minor hysteresis loops for the FePt films. A small shoulder is observed in the hysteresis curve.

The initial magnetization also exhibited a response characteristic of nucleation followed by strong pinning. The initial nucleation response may be due to a small fraction of remaining disordered phase (or less ordered phase) or misoriented grains that can act as easy nucleation sites. This small nucleation response is reversible after removing the applied field [DCD curve, Fig. 2(a)]. Remanent and coercive squareness are ~0.95 and >0.90, respectively. δM curve [Fig. 2(c)] showed a large deviation from the Stoner–Wohlfarth (S–W) relation and strong exchange coupling. The approximate intrinsic anisotropy field (H_k) was ~40 kOe for the hard axis hysteresis loop for FePt films and H_c/H_k can be estimated to be ~0.2. The same size of substrate without any magnetic layer was used to remove the linear background. However, more careful measurements using high field with high sensitivity as well as torque measurement are required to obtain the anisotropy constant.

Analysis of the proposed pinning mechanism is based on microstructural observations of defects. These films have been observed to have only one structural variant in a grain and no structural twins, but there is a possibility of anti-phase boundaries (APB). However, considering the ratio of the defect size (APB and grain boundary) and domain wall width (δ) is ~ 0.1 (APB or grain boundary ~ 0.3–0.4 nm, $\delta \sim 3$–4 nm [1]), the conventional pinning theories [6], [7] reflect the weak pinning mechanism and $H_c <$ ~0.1 H_k.

Fig. 3 illustrates the measured angular dependence of coercivity (H_c) and remanent coercivity (H_{rc} ~ equivalent to the switching field). The measured and simulated angular dependence of H_c and H_{rc} for FePt samples is drawn in Fig. 3(a). We have used the S–W model and micromagnetic (MM) calculation [8], [9] using the measured parameters of K_u (from hard axis, H_k), M_s and d (grain size) as 1.8×10^7 erg/cc, 900 emu/cc and 10 nm, assuming the coherent rotation in a grain and A (exchange stiffness) as 10^{-6} erg/cm [1]. The reduced coercivity can be qualitatively explained by exchange coupling and magnetostatic interactions. The angular dependence of H_c cannot be explained by these models (S–W, MM model) and also does not follow the $1/\cos\omega$ of domain wall motion [Fig. 3(b)]. Therefore, neither coherent rotation in a grain nor pure domain wall motion seems to be occurring in these films. The very small particles (≪the critical monodomain size) may show the incoherent reversal process that involves nucleation and growth

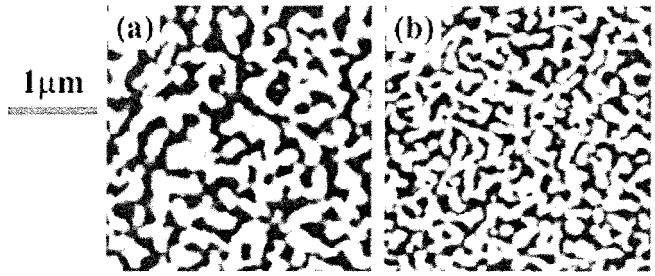

Fig. 4. MFM images of (a) FePt and (b) CoPt 5 nm films (size: 3 μm × 3 μm, thermally demagnetized state).

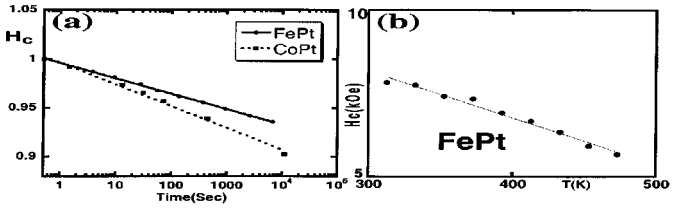

Fig. 5. (a) Time dependence of H_c for CoPt and FePt 5 nm films. (b) Temperature dependence of H_c from ambient temperature to 473 °K.

processes even in a grain due to defects [10]. Although the angular dependence of H_c does not show any unique characteristics [Fig. 3(a), (b)] the trend of H_{rc} in angular dependence seems to follow the trend of the incoherent reversal process [11]. Fig. 4 shows magnetic domain images for FePt and CoPt films. The average domain size is several hundred nanometers.

For thermally activated reversal processes the measured H_c is not an intrinsic property, but depends upon time. To investigate the thermal stability of the magnetization and the activation volume for switching, this time-dependent H_c was measured. The experimental procedure consisted of saturating the samples followed by ($t = 0$) applying a step function reversal field. When the magnetization reaches zero, for a particular field, the time was recorded. By repeating this procedure at many field values the time dependence of H_c was obtained. The activation volume V_{act} was determined from the fluctuation field, H_f, using the relation: $V_{act} = k_B T/M_s H_f$ [12]. The fluctuation field H_f is determined from the measurement of H_c vs $\ln(t)$ using the relationship $t = t_0 \exp[-(H_c - H_0)/H_f]$ (H_0 is a reference field) [13]. From the slope of H_c vs. $\ln(t)$, H_f and V_{act} are obtained. Fig. 5(a) illustrates $H_c(t)$ normalized by H_c at 0.5 second. These samples exhibit thermal decay in our measurement time frame. The V_{act} obtained in this experiment is $\sim 0.4 \times 10^{-18}$ and 0.5×10^{-18} cm^3 for FePt and CoPt samples annealed at 700 °C for 18 min. (using the measured M_s values of ∼900 and ∼600 emu/cc, respectively). Therefore, the V_{act} was found to be larger than some grains but smaller than most of the grains. Given the grain size distribution (average grain size ∼10 nm for FePt) we suggest the possibility of an incoherent reversal process especially for the larger grains (Coherent radius or $l_{ex} = A^{1/2}/M_s$ for FePt ∼10 nm but defects further decrease the coherent radius [10]) and the coupling of clusters of very small grains. The activation volumes are also close to δ^3 (wall width $\delta \sim$ 3–4 nm [1]) and therefore, we cannot exclude the possibility of wall motion and pinning in the grain boundaries.

Fig. 5(b) illustrates the temperature dependence of H_c. The temperature dependence of H_c in thin-film ferromagnets has two limiting cases. The first one is magnetically decoupled particle where the energy barrier to magnetic reversal can be thermally activated [11]. The second is a continuous film where the ferromagnetic domain walls are pinned by a random array of inhomogeneities [14]. During the unpinning process "strong or weak" pinning situations have the different activation energies required to unpin a domain wall [14]. FePt films seem to show a weak pinning mechanism [14] based on the linear relationship between H_c and T (the best fit based on correlation coefficient). However, careful measurements on temperature dependence of K_1 and M_s are required for a more definite demonstration of this.

REFERENCES

[1] D. Weller, A. Moser, L. Folks, M. E. Best, L. Wen, M. F. Toney, M. Schwickert, J.-U. Thiele, and M. F. Doerner, "High Ku materials approach to 100 Gbits/in^2," *IEEE Trans. Magn.*, vol. 36, pp. 10–15, 2000.

[2] D. J. Sellmyer, M. Yu, R. A. Thomas, Y. Liu, and R. D. Kirby, "Nanoscale density of films for extremely high density magnetic recording," *Phys. Low-Dim. Struct.*, vol. 1/2, p. 155, 1998.

[3] T. Suzuki, N. Honda, and K. Ouchi, "Magnetization reversal process in polycrystalline ordered Fe–Pt (001) thin films," *J. Appl. Phys.*, vol. 85, p. 4301, 1999.

[4] S. Jeong, Y.-N. Hsu, D. E. Laughlin, and M. E. McHenry, "Structure and magnetic properties of $L1_0$ CoPt(Ag/MgO, MgO) thin films," *J. Appl. Phys.*, vol. 87, pp. 6950–6952, 2000.

[5] ——, "Atomic ordering and coercivity mechanism in CoPt and FePt polycrystalline thin films," in MMM/Intermag Conference, San Antonio, 2001, submitted for publication.

[6] B. Zhang, "Phase transformation and interrelationship between microstructure, domain structure and magnetic properties in polytwinned FePt and FePd alloys," Ph.D. dissertation, Univ. of Pittsburgh, 1991.

[7] J. M. D. Coey, *Rare-Earth Iron Permanent Magnets*. Oxford: Oxford Science, 1996, pp. 218–282.

[8] P.-L. Lu, "Simulation study of thin film media for high density recording," Ph.D. dissertation, Carnegie Mellon Univ., 1995.

[9] J. G. Zhu, "Interactive phenomena in magnetic thin films," Ph.D. dissertation, Univ. of California (UCSD), 1989.

[10] R. Skomski, J. P. Liu, and D. J. Sellmyer, "Permanent magnetism in exchange-coupled nanocomposites," *Mat. Res. Soc. Proc.*, vol. 577, pp. 335–346, 1999.

[11] Y. Chen, "Microstructural and magnetic properties of barium ferrite thin film recording media," Ph.D. dissertation, Carnegie Mellon Univ., 1998.

[12] E. P. Wohlfarth, "The coefficient of magnetic viscosity," *J. Phys.*, vol. F14, pp. L155–L159, 1984.

[13] R. W. Chantrell, G. N. Coverdale, and K. O'Grady, "Time dependence and rate dependence of the coercivity of particulate recording media," *J. Phys.*, vol. D21, pp. 1469–1471, 1988.

[14] P. Gaunt, "Ferromagnetic domain wall pinning by a random array of inhomogeneities," *Philos. Mag. B*, vol. 48, pp. 261–276, 1983.